Available online at www.sciencedirect.com
ScienceDirect
Biochimica et Biophysica Acta 1768 (2007) 324–335
Biochimica et Biophysica Acta
BBA
www.elsevier.com/locate/bbamem

Hydrogen-bond formation of the residue in H-loop of the nucleotide binding domain 2 with the ATP in this site and/or other residues of multidrug resistance protein MRP1 plays a crucial role during ATP-dependent solute transport

Runying Yang, Xiu-bao Chang *

Mayo Clinic College of Medicine, Mayo Clinic Arizona, 13400 East Shea Boulevard, Scottsdale, AZ 85259, USA

Received 21 June 2006; received in revised form 12 October 2006; accepted 14 November 2006
Available online 18 November 2006

Abstract

MRP1 couples ATP binding/hydrolysis to solute transport. We have shown that ATP binding to nucleotide-binding-domain 1 (NBD1) plays a regulatory role whereas ATP hydrolysis at NBD2 plays a crucial role in ATP-dependent solute transport. However, how ATP is hydrolyzed at NBD2 is not well elucidated. To partially address this question, we have mutated the histidine residue in H-loop of MRP1 to either a residue that prevents the formation of hydrogen-bonds with ATP and other residues in MRP1 or a residue that may potentially form these hydrogen-bonds. Interestingly, substitution of H827 in NBD1 with residues that prevented formation of these hydrogen-bonds had no effect on the ATP-dependent solute transport whereas corresponding mutations in NBD2 almost abolished the ATP-dependent solute transport completely. In contrast, substitutions of H1486 in H-loop of NBD2 with residues that might potentially form these hydrogen-bonds exerted either full function or partial function, implying that hydrogen-bond formation between the residue at 1486 and the γ-phosphate of the bound ATP and/or other residues, such as putative catalytic base E1455, together with S769, G771, T1329 and K1333, etc., holds all the components necessary for ATP binding/hydrolysis firmly so that the activated water molecule can efficiently hydrolyze the bound ATP at NBD2.

Keywords: MRP1; Nucleotide binding domain (NBD); ATP binding/hydrolysis; Hydrogen-bond; ATP-dependent solute transport

1. Introduction

Cells over-expressing P-glycoprotein (P-gp or ABCB1) [1,2], breast cancer resistance protein (BCRP or ABCG2) [3,4] and/or multidrug resistance protein (MRP1 or ABCC1) [5,6] are resistant to a broad range of anticancer drugs. P-gp is a 170 kDa membrane-bound glycoprotein with two transmembrane domains (TMD) and two nucleotide binding domains (NBD) [2,7,8]. MRP1 is a 190 kDa membrane-bound glycoprotein with a core structure of P-gp and an extra N-terminal domain composed of TMD_0 and L_0 linker region [6,9,10]. BCRP is a 72 kDa membrane-bound protein with an NBD followed by a TMD with six transmembrane segments [3,4,11,12]. Although the topology of BCRP is somewhat different from P-gp or MRP1 as it has only half of the core structure of P-gp [3,4,11,12], the functional unit of BCRP is a homodimer with two TMDs and two NBDs [13–18]. Thus, although their molecular weights, amino acid compositions and topologies are different, these ATP-binding cassette (ABC) transporters share a common architecture composed of two NBDs and two TMDs, which are believed to be used to couple ATP binding/hydrolysis to anticancer drug transport.

Sequence dissimilarities between NBD1 and NBD2 of MRP1 protein imply that they may play different roles during ATP-dependent solute transport. Indeed, substitution of the

Abbreviations: BHK, baby hamster kidney; Sf21, Spodoptera frugiperda 21; ABC, ATP binding cassette; MRP1, multidrug resistance protein; P-gp, P-glycoprotein; NBD, nucleotide binding domain; LTC4, leukotriene C4; 8-N_3ATP, 8-azidoadenosine 5′-triphosphate; EGTA, ethylene glycol-bis(β-aminoethyl ether)*N*,*N*,*N*,*N*-tetraacetic acid; SDS, sodium dodecyl sulfate; X-gal, 5-bromo-4-chloro-indolyl-β-D-galactoside and IPTG, isopropylthio-β-D-galactoside

* Corresponding author. Tel.: +1 480 301 6206; fax: +1 480 301 7017.
E-mail address: xbchang@mayo.edu (X. Chang).

0005-2736/$ - see front matter © 2006 Elsevier B.V. All rights reserved.
doi:10.1016/j.bbamem.2006.11.009

essential positive charged lysine residue in Walker A motif in NBD2 with a non-charged amino acid abolished the ATP-dependent solute transport activity completely, whereas the corresponding substitution in NBD1 decreased the transport activity to approximately half of wild-type MRP1 [19,20]. In addition, it has been found that NBD1 has a higher affinity for ATP than that of NBD2 [21]. Thus, ATP binding to NBD1 and NBD2 of MRP1 protein should be a sequential event. Once ATP is bound to NBD1, it induces conformational changes of the protein and enhances ATP binding to NBD2 [22]. If mutation in NBD1 significantly impairs ATP binding at the mutated NBD1, it also severely affects the ATP binding at the un-mutated NBD2 [23], implying that ATP binding at NBD1 plays an important role during the NBD1·ATP·ATP·NBD2 heterodimer sandwich formation [24]. However, ATP hydrolysis at the NBD1 seems likely not essential since substitution of the putative catalytic base D793 in NBD1 with a non-acidic amino acid does not significantly affect the ATP-dependent solute transport [25,26]. Conversely, substitution of the putative catalytic base E1455 in NBD2 with a non-acidic amino acid almost abolished the ATP-dependent solute transport activity completely [25,26], implying that ATP hydrolysis at the NBD2 of MRP1 is essential.

However, it is still not clear why some of the NBD2 mutations significantly decreased the affinity for ATP at the mutated NBD2 and ATP-dependent solute transport activity, whereas other NBD2 mutations significantly decreased the affinity for ATP, but increased the ATP-dependent solute transport activity. For example, replacement of the aromatic Y1302 residue, which should interact with the adenine ring of the bound ATP, with a polar cysteine residue that significantly decreased the affinity for ATP at the mutated NBD2, but increased the ATP-dependent solute transport activity [27]. In contrast, mutations of the residue that should interact with the γ-phosphate of the bound ATP [28,29], such as K1333L [20], significantly decreased the ATP binding at the mutated NBD2 [23] and almost abolished the ATP-dependent solute transport activity completely. Accordingly, mutations of the residues that should interact with the γ-phosphate of the bound ATP [28,29], such as K1333M [19] or G771A [30], also almost abolished the ATP-dependent solute transport activity completely. Thus, we speculated that the hydrogen-bond formation between the residues involved in ATP binding and the γ-phosphate of the bound ATP in NBD2 might play an important role during the ATP hydrolysis. In this report we have mutated the histidine residue in H-loop to either a residue that prevents the formation of hydrogen-bonds with ATP and other residues in MRP1 or a residue that may potentially form these hydrogen-bonds and found that hydrogen-bond formation between the histidine residue in H-loop of NBD2 and the γ-phosphate of the bound ATP and/or other residues plays a crucial role during the ATP hydrolysis at NBD2 and ATP-dependent solute transport.

2. Materials and methods

2.1. Materials

Sodium orthovanadate, EGTA, isopropylthio-β-D-galactoside (IPTG), 5-bromo-4-chloro-indolyl-β-D-galactoside (X-gal) and ATP were purchased from Sigma. [α-^{32}P]-8-N_3ATP and [γ-^{32}P]-8-N_3ATP were purchased from Affinity Labeling Technologies. ([14,15,19,20-^{3}H)-leukotriene C4 (LTC4) was from NEN Life Science Products. CellFECTIN reagent, DMEM/F12 medium and Grace's insect cell culture medium were from Invitrogen. Fetal bovine serum was from Gemini Bio-Products. Stratalinker UV Crosslinker 2400 model (wavelength 254 nm) and QuikChange site-directed mutagenesis kit were from Stratagene. Chemiluminescent substrates were from Pierce.

2.2. Generation of constructs

N-half (1–932) and C-half (933–1531) of human MRP1 cloned into pDual expression vector [26] was used as a template for the in vitro mutagenesis. The histidine residue at position of 827 or 1486 was mutated to either leucine or phenylalanine (Fig. 1A, H827L, H827F, H1486L or H1486F) by using the forward/reverse primers and the QuikChange site-directed mutagenesis kit from Stratagene [20]. The forward and reverse primers for these mutations are: H827L/forward, 5′-CGG ATC TTG GTC ACG CTC AGC ATG AGC TAC TTG-3′; H827L/reverse, 5′-CAA GTA GCT CAT GCT GAG CGT GAC CAA GAT CCG-3′; H1486L/forward, 5′-GTC CTC ACC ATC GCC CTC CGG CTC AAC ACC ATC-3′; H1486L/reverse, 5′-GAT GGT GTT GAG CCG GAG GGC GAT GGT GAG GAC-3′; H827F/forward, 5′-CGG ATC TTG GTC ACG TTC AGC ATG AGC TAC TTG-3′; H827F/reverse, 5′-CAA GTA GCT CAT GCT GAA CGT GAC CAA GAT CCG-3′; H1486F/forward, 5′-GTC CTC ACC ATC GCC TTC CGG CTC AAC ACC ATC-3′; H1486F/reverse, 5′-GAT GGT GTT GAG CCG GAA GGC GAT GGT GAG GAC-3′. These mutations (Fig. 4A, H827L, H827F, H1486L, H1486F, H827L/H1486L or H827F/H1486F) were also introduced into full length MRP1 cDNA by using the QuikChange site-directed mutagenesis kit [20] with the plasmid DNA pNUT/MRP1/His [31] as a template and the forward/reverse oligonucleotides shown above as primers. In addition, the following mutations as shown in Fig. 5A (H827D, H1486D, H827D/H1486D, H827N, H1486N, H827N/H1486N, H827E, H1486E, H827E/H1486E, H827Q, H1486Q, H827Q/H1486Q, H827Y, H1486Y, H827Y/H1486Y, H827W, H1486W and H827W/H1486W) were also introduced into the full length MRP1 cDNA by using the following primers: H827D/forward, 5′-CGG ATC TTG GTC ACG GAC AGC ATG AGC TAC TTG-3′; H827D/reverse, 5′-CAA GTA GCT CAT GCT GTC CGT GAC CAA GAT CCG-3′; H1486D/forward, 5′-GTC CTC ACC ATC GCC GAC CGG CTC AAC ACC ATC-3′; H1486D/reverse, 5′-GAT GGT GTT GAG CCG GTC GGC GAT GGT GAG GAC-3′; H827N/forward, 5′-CGG ATC TTG GTC ACG AAC AGC ATG AGC TAC TTG-3′; H827N/reverse, 5′-CAA GTA GCT CAT GCT GTT CGT GAC CAA GAT CCG-3′; H1486N/forward, 5′-GTC CTC ACC ATC GCC AAC CGG CTC AAC ACC ATC-3′; H1486N/reverse, 5′-GAT GGT GTT GAG CCG GTT GGC GAT GGT GAG GAC-3′; H827E/forward, 5′-CGG ATC TTG GTC ACG GAG AGC ATG AGC TAC TTG-3′; H827E/reverse, 5′-CAA GTA GCT CAT GCT CTC CGT GAC CAA GAT CCG-3′; H1486E/forward, 5′-GTC CTC ACC ATC GCC GAG CGG CTC AAC ACC ATC-3′; H1486E/reverse, 5′-GAT GGT GTT GAG CCG CTC GGC GAT GGT GAG GAC-3′; H827Q/forward, 5′-CGG ATC TTG GTC ACG CAG AGC ATG AGC TAC TTG-3′; H827Q/reverse, 5′-CAA GTA GCT CAT GCT CTG CGT GAC CAA GAT CCG-3′; H1486Q/forward, 5′-GTC CTC ACC ATC GCC CAG CGG CTC AAC ACC ATC-3′; H1486Q/reverse, 5′-GAT GGT GTT GAG CCG CTG GGC GAT GGT GAG GAC-3′; H827Y/forward, 5′-CGG ATC TTG GTC ACG TAC AGC ATG AGC TAC TTG-3′; H827Y/reverse, 5′-CAA GTA GCT CAT GCT GTA CGT GAC CAA GAT CCG-3′; H1486Y/forward, 5′-GTC CTC ACC ATC GCC TAC CGG CTC AAC ACC ATC-3′; H1486Y/reverse, 5′-GAT GGT GTT GAG CCG GTA GGC GAT GGT GAG GAC-3′; H827W/forward, 5′-CGG ATC TTG GTC ACG TGG AGC ATG AGC TAC TTG-3′; H827W/reverse, 5′-CAA GTA GCT CAT GCT CCA CGT GAC CAA GAT CCG-3′; H1486W/forward, 5′-GTC CTC ACC ATC GCC TGG CGG CTC AAC ACC ATC-3′; H1486W/reverse, 5′-GAT GGT GTT GAG CCG CCA GGC GAT GGT GAG GAC-3′. The underlined sequences are codons for mutated residues. The regions containing these mutations were sequenced to confirm that the correct clones were obtained.

2.3. Cell culture and cell lines expressing MRP1

Baby hamster kidney (BHK-21) cells were cultured in DMEM/F12 medium supplemented with 5% fetal bovine serum at 37 °C in 5% CO_2.

Subconfluent cells were transfected with pNUT-MRP1/His in the presence of 20 mM HEPES (pH 7.05), 137 mM NaCl, 5 mM KCl, 0.7 mM Na_2HPO_4, 6 mM dextrose and 125 mM $CaCl_2$ [31]. Surviving individual colonies in media containing 200 μM methotrexate were picked and amplified. Cells for membrane vesicle preparation were grown in DMEM/F12 media containing 5% fetal bovine serum and 200 μM methotrexate in roller bottles (on a roller machine from BELLCO). Spodoptera frugiperda 21 (Sf21) cells were cultured in Grace's insect cell medium supplemented with heat-inactivated 5% fetal bovine serum at 27 °C. Viral infection was performed according to Invitrogen's recommendation.

2.4. Recombinant viral DNA preparation and viral particle production

Generation of recombinant viral DNA was performed according to Invitrogen's recommendation. pDual/N-half/C-half donor plasmid DNA was transformed into DH10Bac competent cells harboring the parent Bacmid DNA with a mini-attTn7 target site and the helper plasmid. Bacteria transformed with the donor plasmid DNA were selected on LB plates containing 50 μg/ml kanamycin, 7 μg/ml gentamicin and 10 μg/ml tetracycline. In addition, colonies containing recombinant Bacmids were identified by disruption of the lacZα gene (white colonies) on the LB plates containing 100 μg/ml X-gal and 40 μg/ml IPTG. A single colony confirmed as having a white phenotype on the LB plate with X-gal and IPTG was inoculated in medium containing 50 μg/ml kanamycin, 7 μg/ml gentamicin and 10 μg/ml tetracycline. The purified recombinant Bacmids were confirmed by polymerase chain reaction with MRP1 specific primers and then used to transfect Sf21 cells with CellFECTIN reagent. After 3–4 days incubation at 27 °C, the supernatants containing viral particles were collected and the cells were lysed with 2% SDS, separated on a 7% polyacrylamide gel, electro-blotted to a nitrocellulose membrane and probed with MRP1-specific monoclonal antibodies 42.4 and 897.2 [20].

2.5. Viral plaque assay and viral infection

Viral plaque assay was performed according to Invitrogen's recommendation. The expression levels of the dual-expressed N-halves and C-halves with varying multiplicity of infection (MOI) were determined by Western blot. MOI of 8 was used to infect Sf21 cells for membrane vesicle preparations.

2.6. Identification of MRP1 protein

Western blot was performed according to the method described previously [20]. 42.4 monoclonal antibody was used to identify the NBD1-containing N-half fragment of MRP1, whereas 897.2 monoclonal antibody was used to detect the NBD2-containing C-half fragment [20,27]. The secondary antibody used was anti-mouse Ig conjugated with horse radish peroxidase. Chemiluminescent film detection was performed according to the manufacturer's recommendations (Pierce).

2.7. Membrane vesicle preparations

Membrane vesicles were prepared according to the procedure described previously [20]. The membrane vesicle pellet was re-suspended in a solution containing 10 mM Tris–HCl (pH 7.5), 250 mM sucrose and 1× protease inhibitors (2 μg/ml aprotinine, 121 μg/ml benzamidine, 3.5 μg/ml E64, 1 μg/ml leupeptin and 50 μg/ml Pefabloc). After passage through a Liposofast™ vesicle extruder (Avestin, Ottawa, Canada) they were divided into 200 μl aliquots and stored in −80 °C.

2.8. Membrane vesicle transport

ATP-dependent LTC4 transport was assayed by a rapid filtration technique [32,33]. Briefly, 30 μl solution containing 3 μg of membrane proteins, 50 mM Tris–HCl (pH 7.5), 250 mM sucrose, 10 mM $MgCl_2$, 200 nM LTC4 (17.54 nCi of ^{3}H-labeled LTC4) and 4 mM ATP (4 mM AMP was used as control) were mixed on ice and then incubated at 37 °C for 4 min. The samples were brought back to ice, diluted with 1 ml of ice-cold 1× transport buffer (50 mM Tris–HCl, pH 7.5, 250 mM sucrose and 10 mM $MgCl_2$) immediately and trapped on nitrocellulose membranes (0.2 μm) that had been equilibrated with 1× transport buffer. The filter was then washed with 10 ml of ice-cold 1× transport buffer, air-dried and placed in a 10 ml of biodegradable counting scintillant (Amersham Pharmacia Biotech). The radioactivity bound to the nitrocellulose membrane was determined by liquid scintillation counting (Beckman LS 6000SC).

2.9. Photoaffinity labeling of MRP1 protein

Vanadate (Vi) preparation and photoaffinity labeling of MRP1 protein were performed according to procedures described previously [20]. Briefly, photolabeling experiments were carried out in a 10 μl solution containing 10 μg membrane vesicles, 40 mM Tris–HCl (pH 7.5), 2 mM ouabain, 10 mM $MgCl_2$ and 0.1 mM EGTA. Concentration of ^{32}P-labeled nucleotide, Vi, incubation time and temperature are specifically indicated in Figs. 2 and 3. The labeled proteins were separated by polyacrylamide gel (7%) electrophoresis and electro-blotted to a nitrocellulose membrane.

2.10. Statistical analysis

The results in Tables 1 and 2 were presented as means±S.D. from three (Table 1) or four (Table 2) independent experiments. The two-tailed P values were calculated based on the unpaired t test from GraphPad Software Quick Calcs. By conventional criteria, if P value is less than 0.05, the difference between two samples is considered to be statistically significant.

3. Results

3.1. Substitution of H827 in H-loop of NBD1 with an amino acid that prevents formation of the hydrogen-bond with the γ-phosphate of the bound ATP has no effect on the ATP-dependent LTC4 transport whereas corresponding mutation in NBD2 almost abolishes the ATP-dependent LTC4 transport activity completely

Structural analyses of bacterial ABC transporter NBDs revealed that the histidine residue in H-loop contributes to

Table 1
Mean K_d (8-N_3ATP) values of wild-type and mutant MRP1

Samples		K_d [a] of NBD1 (μM 8-N_3ATP)	K_d of NBD2 (μM 8-N_3ATP)
N-half	C-half		
Wild-type	Wild-type	11.7±2.7	32.4±2.5
H827L	Wild-type	59.5±0.5 [b]	60.0±3.0
Wild-type	H1486L	31.0±0.8	58.7±1.3
H827L	H1486L	59.7±1.3	53.0±0.8
H827F	Wild-type	12.3±0.5	32.7±0.9
Wild-type	H1486F	11.5±0.5	33.0±1.0
H827F	H1486F	58.0±1.0	51.5±0.5

[a] The K_d (8-N3ATP) values (n=3) of wild-type and mutant MRP1s were derived from Fig. 2. The amount of [α-^{32}P]-8-N_3ATP incorporated into the N-half (NBD1) or C-half (NBD2) fragment was measured by Packard Instant Imager and plotted out against [α-^{32}P]-8-N_3ATP concentration. K_d is calculated by using the formula: $K_d=(L_{max}-L)[S]/L$, where [S] is the concentration of [α-^{32}P]-8-N_3ATP, L is the amount of [α-^{32}P]-8-N_3ATP labeled on NBD1 or NBD2 and L_{max} is the maximum amount of [α-^{32}P]-8-N_3ATP labeled on NBD1 or NBD2.

[b] Statistical analysis indicated that the K_d values of NBD1 from H827L, H1486L, H827L/H1486L and H827F/H1486F or the K_d values of NBD2 from H827L, H1486L, H827L/H1486L and H827F/H1486F are significantly different from that of wild-type NBD1 (11.7 μM 8-N_3ATP) or wild-type NBD2 (32.4 μM 8-N_3ATP). In contrast, the K_d values of NBD1 or NBD2 from H827F or H1486F are not significantly different from that of wild-type NBD1 (11.7 μM 8-N_3ATP) or wild-type NBD2 (32.4 μM 8-N_3ATP).

Table 2
Ratio of [γ-^{32}P]-8N_3ATP/[α-^{32}P]-8N_3ATP labeling at NBD1 or NBD2

Samples		Ratio [a] at NBD1	Ratio at NBD2
N-half	C-half		
Wild-type	Wild-type	2.12±0.26 [b]	0.70±0.14
H827L	Wild-type	1.92±0.45	0.90±0.02
Wild-type	H1486L	1.89±0.34	1.26±0.12
H827L	H1486L	2.12±0.32	1.38±0.33
H827F	Wild-type	2.17±0.15	0.93±0.02
Wild-type	H1486F	2.15±0.10	1.42±0.14
H827F	H1486F	1.98±0.20	1.42±0.19

[a] The ratio (n=4) of [γ-^{32}P]-8-N_3ATP/[α-^{32}P]-8-N_3ATP labeling at NBD1 or NBD2 was derived from Fig. 3. The amount of ^{32}P-8-N_3ATP incorporated into the N-half (NBD1) or C-half (NBD2) fragment was measured by employing Packard Instant Imager. The ratio of [γ-^{32}P]-8-N_3ATP/[α-^{32}P]-8-N_3ATP labeling at NBD1 or NBD2 was calculated by dividing the amount of [γ-^{32}P]-8-N_3ATP labeling with that of [α-^{32}P]-8-N_3ATP labeling.

[b] Statistical analysis indicated that the ratio values of NBD1 from all the mutants are not significantly different from that of wild-type NBD1 (2.12). The ratio values of NBD2 from H827L and H827F are also not significantly different from that of wild-type NBD2. In contrast, the ratio values of NBD2 from H1486L, H827L/H1486L, H1486F and H827F/H1486F are significantly different from that of wild-type NBD2 (0.70).

ATP binding by interacting with the γ-phosphate of the bound ATP [28,34,35] and to ATP hydrolysis by interacting with the putative catalytic base to form the "catalytic dyad" [29]. Alignment of amino acid sequences in NBDs indicates that majority of the ABC transporters conserves the histidine residue in H-loop [28] downstream of the Walker B motif. However, there are some exceptions, such as a Y in NBD1 of pDR5 [36], a Q in TAP1 [37], an N in NBD1 of YCF1 [38] and an S in NBD1 of CFTR [39], implying that these residues in H-loop, including Y, Q, N or S, might have a potential to form hydrogen-bonds with the γ-phosphate of the bound ATP and the putative catalytic base to form the "catalytic dyad".

In order to test the functional role of these hydrogen-bond formations between the histidine residue in H-loop and the components mentioned above, this histidine residue was substituted with a residue that could abolish the formation of this hydrogen-bond, such as a leucine (L) residue or a phenylalanine (F) residue (Fig. 1A). These mutants made in N-half, including H827L or H827F in NBD1, or in C-half, including H1486L or H1486F in NBD2 or H827L/H1486L and H827F/H1486F in N-half and C-half, were expressed simultaneously in Sf21 insect cells. The results in Fig. 1B indicated that both N-half and C-half of MRP1 proteins were expressed simultaneously. Membrane vesicles prepared from Sf21 cells infected with viral particles containing variant mutants and pDual vector (used as a control) were used for ATP-dependent LTC4 transport assay (Fig. 1C). Mutations at NBD1, including H827L and H827F, did not have a significant effect on the ATP-dependent LTC4 transport, whereas mutations at NBD2, including H1486L, H1486F, H827L/H1486L and H827F/H1486F, greatly decreased the ATP-dependent LTC4 transport activity (Fig. 1C).

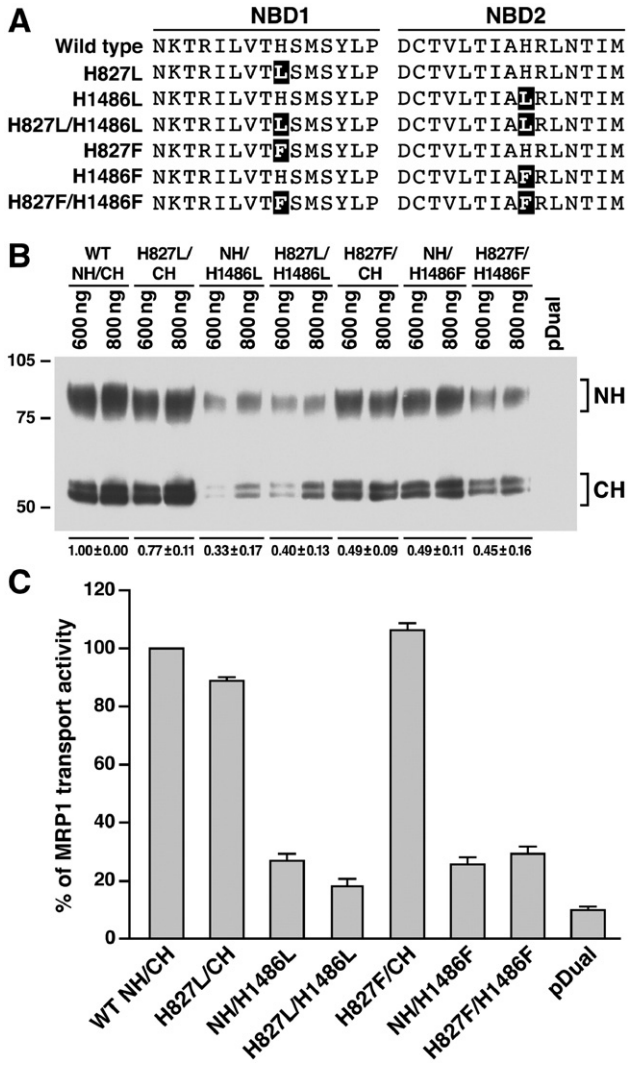

Fig. 1. Substitution of H1486 in NBD2 with either a leucine or a phenylalanine significantly decreases the ATP-dependent LTC4 transport activity. (A) Substitution of histidine residue at H827 or H1486 with either a leucine (L) or a phenylalanine (F). The highlighted letters indicate that the histidine residue was substituted with either an L or an F at that position. The definition of H827L means that the H827L-mutated N-half is co-expressed with wild-type C-half, whereas H1486L means that the H1486L-mutated C-half is co-expressed with wild-type N-half. (B) Expression of wild-type and variant mutants of human MRP1 proteins in Sf21 insect cells. Membrane vesicles were prepared from Sf21 cells infected with viral particles containing either wild-type or variant mutants of human MRP1. The amounts of membrane vesicle protein loaded in the gel are indicated on the top. Molecular weight markers are indicated on the left. NH and CH on the right indicate the N-proximal half and the C-proximal half of MRP1 proteins that were detected in western blot by employing the monoclonal antibody 42.4 against NBD1 and 897.2 against NBD2. The intensities of the N-half and C-half bands were determined by a scanning densitometer. The mean ratios (n=3), considering the amount of wild type N-half and C-half of MRP1 as 1, of the mutant proteins including N-half and C-half in the membrane vesicles are listed at the bottom of the gel. (C) Relative rate of ATP-dependent LTC4 transport activity. The assays were carried out in a 30 μl solution containing 3 μg of membrane vesicles (the amount of MRP1 protein determined in B was adjusted to a similar amount by adding varying amount of membrane vesicles prepared from Sf21 cells infected with pDual expression vector) and 4 mM AMP (used as a control) or 4 mM ATP at 37 °C for 4 min. The amount of LTC4 bound to the membrane vesicles in the presence of 4 mM AMP was subtracted from the corresponding samples in the presence of 4 mM ATP. The data are means±S.D. of four triplicate-determinations.

3.2. Substitution of the imidazole ring in histidine residue in H-loop with a benzene ring in phenylalanine did not significantly affect ATP binding, whereas substitution of this histidine residue with a hydrophobic leucine significantly decreased the affinity for 8-N_3ATP

Since histidine residue in H-loop forms hydrogen-bond with the γ-phosphate of the bound ATP and contributes to the ATP binding, substitution of this histidine residue with an amino acid that prevents formation of hydrogen-bond with the γ-phosphate of the bound ATP should decrease the affinity for ATP at the mutated site. In order to test this hypothesis, membrane vesicles containing wild type or variant mutants were used to label with [α-^{32}P]-8-N_3ATP on ice (Fig. 2). Since the labeling on ice mainly reflects the equilibrium of the following forwarding and reversing reactions:

$$[\alpha\text{-}^{32}\text{P}]\text{-8-N}_3\text{ATP} + \text{NBD} \underset{k_{-1}}{\overset{k_1}{\rightleftharpoons}} [\alpha\text{-}^{32}\text{P}]\text{-8-N}_3\text{ATP} \cdot \text{NBD}$$

where the velocity of forwarding reaction $v_f = k_1\{\text{NBD}\}\{[\alpha\text{-}^{32}\text{P}]\text{-8-N}_3\text{ATP}\}$ and the velocity of reversing reaction $v_r = k_{-1}\{[\alpha\text{-}^{32}\text{P}]\text{-8-N}_3\text{ATP}\cdot\text{NBD}\}$. At the equilibrium, the velocity of forwarding reaction v_f equals to the velocity of reversing reaction v_r, thus, $k_1\{\text{NBD}\}\{[\alpha\text{-}^{32}\text{P}]\text{-8-N}_3\text{ATP}\} = k_{-1}\{[\alpha\text{-}^{32}\text{P}]\text{-8-N}_3\text{ATP}\cdot\text{NBD}\}$, $k_{-1}/k_1 = \{\text{NBD}\}\{[\alpha\text{-}^{32}\text{P}]\text{-8-N}_3\text{ATP}\}/\{[\alpha\text{-}^{32}\text{P}]\text{-8-N}_3\text{ATP}\cdot\text{NBD}\}$.

The K_d value for each NBD, where $K_d = k_{-1}/k_1$, should reflect the affinity for 8-N_3ATP. Mutation of H827L increased the K_d (8-N_3ATP) value of the mutated NBD1 from 11.7 μM (wild-type NBD1, Fig. 2A and Table 1) to 59.5 μM (Fig. 2B and Table 1), implying that H827L mutation decreased the affinity for 8-N_3ATP at the mutated NBD1. Interestingly, this mutation also increased the K_d (8-N_3ATP) value of NBD2 (60.0 μM, Fig. 2B and Table 1) even though the amino acid sequences in NBD2 were not changed, presumably the decreased ATP binding at the H827L-mutated NBD1 altered the affinity for 8-N_3ATP at the un-mutated NBD2. Accordingly, mutation of H1486L increased the K_d (8-N_3ATP) value of NBD2 from 32.4 μM (wild-type NBD2, Fig. 2A and Table 1) to 58.7 μM (Fig. 2C and Table 1) and the K_d (8-N_3ATP) value of the un-mutated NBD1 from 11.7 μM (wild-type NBD1) to 31 μM (Fig. 2C and Table 1). Thus, it is not surprising that the double mutant H827L/H1486L increased both K_d (8-N_3ATP) values for NBD1 and NBD2 (Fig. 2D and Table 1). However, substitution of this histidine residue in H-loop with an aromatic F residue in either NBD1 (H827F) or NBD2 (H1486F) did not significantly alter the K_d (8-N_3ATP) values at either NBD1 or NBD2 (Fig. 2E, F and Table 1), suggesting that replacement of the five-member imidazole ring with the six-member benzene ring did not significantly alter the local conformation in ATP binding pocket, especially the van der Waals interactions with the residues in D-loop of counterpart NBDs [29], and hydrogen-bond formation between the residue at 827 or 1486 and the γ-phosphate of ATP bound at that site played a minor role for ATP-binding. However, the double mutant H827F/H1486F did significantly increase the K_d (8-N_3ATP) values for the H827F-mutated NBD1 and H1486F-mutated NBD2 (Fig. 2G and Table 1), presumably the tertiary structure alterations caused by these two mutations affect ATP binding at the mutated NBD1 and NBD2.

3.3. Substitution of the H1486 in H-loop with either an L or an F decreased the rate of ATP hydrolysis at the mutated NBD2

Although substitution of H1486 residue in H-loop with an aromatic F residue did not significantly affect 8-N_3ATP binding (Fig. 2F and Table 1), this mutation did significantly decrease the ATP-dependent LTC4 transport (Fig. 1C). Since histidine residue in H-loop may contribute to ATP hydrolysis by interacting with the putative catalytic base to form the "catalytic dyad" [29], we speculated that even though ATP can efficiently bind to the H1486F-mutated NBD2, but the bound ATP cannot be efficiently hydrolyzed. In order to test this hypothesis, these mutated MRP1 proteins in membrane vesicles were labeled with either [α-^{32}P]-8-N_3ATP or [γ-^{32}P]-8-N_3ATP in the presence of vanadate at 37 °C (Fig. 3). In that case, the vanadate-trapped [α-^{32}P]-8-N_3ATP hydrolysis product [α-^{32}P]-8-N_3ADP can still label the NBD whereas the vanadate-trapped [γ-^{32}P]-8-N_3ATP hydrolysis product 8-N_3ADP cannot. Thus, a high ratio of [γ-^{32}P]-8-N_3ATP/[α-^{32}P]-8-N_3ATP labeling at either NBD1 or NBD2 should reflect that ATP bound at that specific NBD was not efficiently hydrolyzed. The ratio (Table 2) of [γ-^{32}P]-8-N_3ATP/[α-^{32}P]-8-N_3ATP labeling at either NBD1 (NH) or NBD2 (CH) was calculated based on the counts in each band (Fig. 3). The ratio of 2.12 in wild-type NBD1 is much higher than the ratio of 0.70 in wild-type NBD2 (Table 2), implying that the ATP bound to the wild-type NBD1 was not efficiently hydrolyzed whereas the ATP bound to the wild-type NBD2 was efficiently hydrolyzed. The ratio of [γ-^{32}P]-8-N_3ATP/[α-^{32}P]-8-N_3ATP labeling at the NBD1, regardless of whether this NBD is mutated or not, is ~ 2 (Table 2), implying that mutation of H827 to either L or F at NBD1 does not have a significant effect on the 8-N_3ATP hydrolysis at this site. In addition, H827L or H827F mutation did not significantly affect the ratio of the un-mutated NBD2 (Table 2), consistent with their high LTC4 transport activities (Fig. 1C). In contrast, however, the ratio of [γ-^{32}P]-8-N_3ATP/[α-^{32}P]-8-N_3ATP labeling at the mutated NBD2, regardless of whether this H residue is mutated to an L or an F, including H1486L, H827L/H1486L, H1486F and H827F/H1486F, is significantly increased (Table 2), implying that the 8-N_3ATP bound to the mutated NBD2 is not efficiently hydrolyzed, consistent with their low LTC4 transport activities (Fig. 1C).

3.4. The non-efficient ATP hydrolysis at the H1486L- or H1486F-mutated NBD2 is not caused by global conformational alterations

Since the N-halves and C-halves were expressed in Sf21 cells at 27 °C, the results derived from western blot in Fig. 1B cannot tell whether these N-halves and C-halves were globally folded properly or not. Thus, although it was clear that 8-N_3ATP bound to the H1486L- or H1486F-mutated NBD2 was not

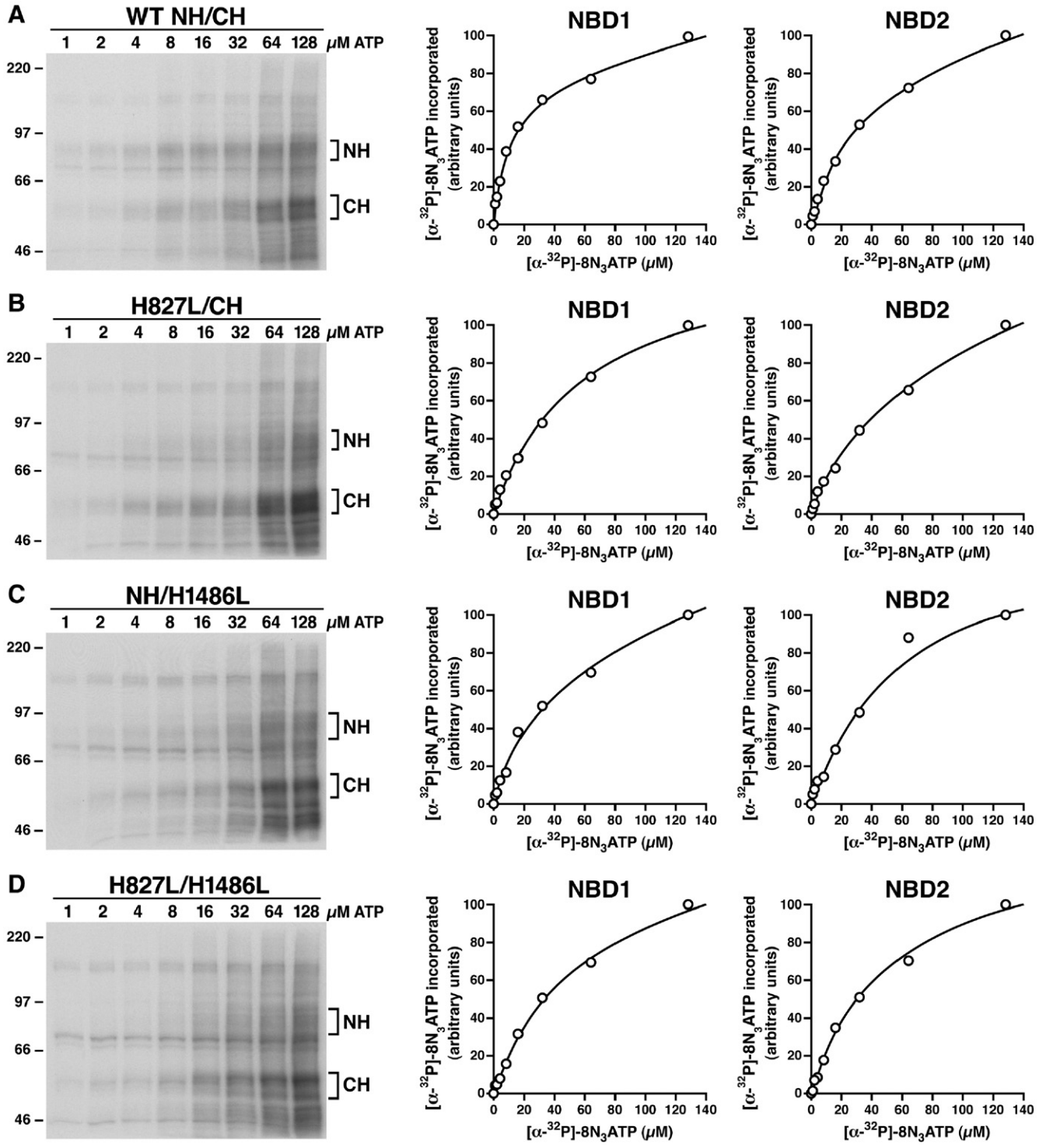

Fig. 2. The effects of H827L, H1486L, H827L/H1486L, H827F, H1486F or H827F/H1486F mutations on 8-N_3ATP binding at NBD1 and NBD2. Membrane vesicles were prepared from Sf21 cells infected with viral particles containing either wild-type or variant mutants of human MRP1. Photolabeling experiments were carried out in a 10 μl of solution containing 10 μg membrane vesicle proteins and varying concentration of [α-^{32}P]-8-N_3ATP on ice for 10 min. The reaction mixture was UV-irradiated on ice for 2 min, subjected to SDS-PAGE (7%) and electroblotted to a nitrocellulose membrane. Panel A shows the autoradiogram of [α-^{32}P]-8-N_3ATP labeled wild-type N-half+wild-type C-half and the plots of the amount of [α-^{32}P]-8-N_3ATP incorporated into wild-type N-half (NBD1) co-expressed with wild-type C-half (NBD2). Panels B, C, D, E, F and G show the results derived from H827L-mutated N-half+wild-type C-half, wild-type N-half+H1486L-mutated C-half, H827L-mutated N-half+H1486L-mutated C-half, H827F-mutated N-half+wild-type C-half, wild-type N-half+H1486F-mutated C-half and H827F-mutated N-half+H1486F-mutated C-half. Molecular weight markers are indicated on the left. NH and CH on the right of the gel indicate the [α-^{32}P]-8-N_3ATP labeled N-half and C-half of MRP1 proteins which were confirmed by western blots by employing the NBD1-specific monoclonal antibody 42.4 [20] and NBD2-specific monoclonal antibody 897.2 [20].

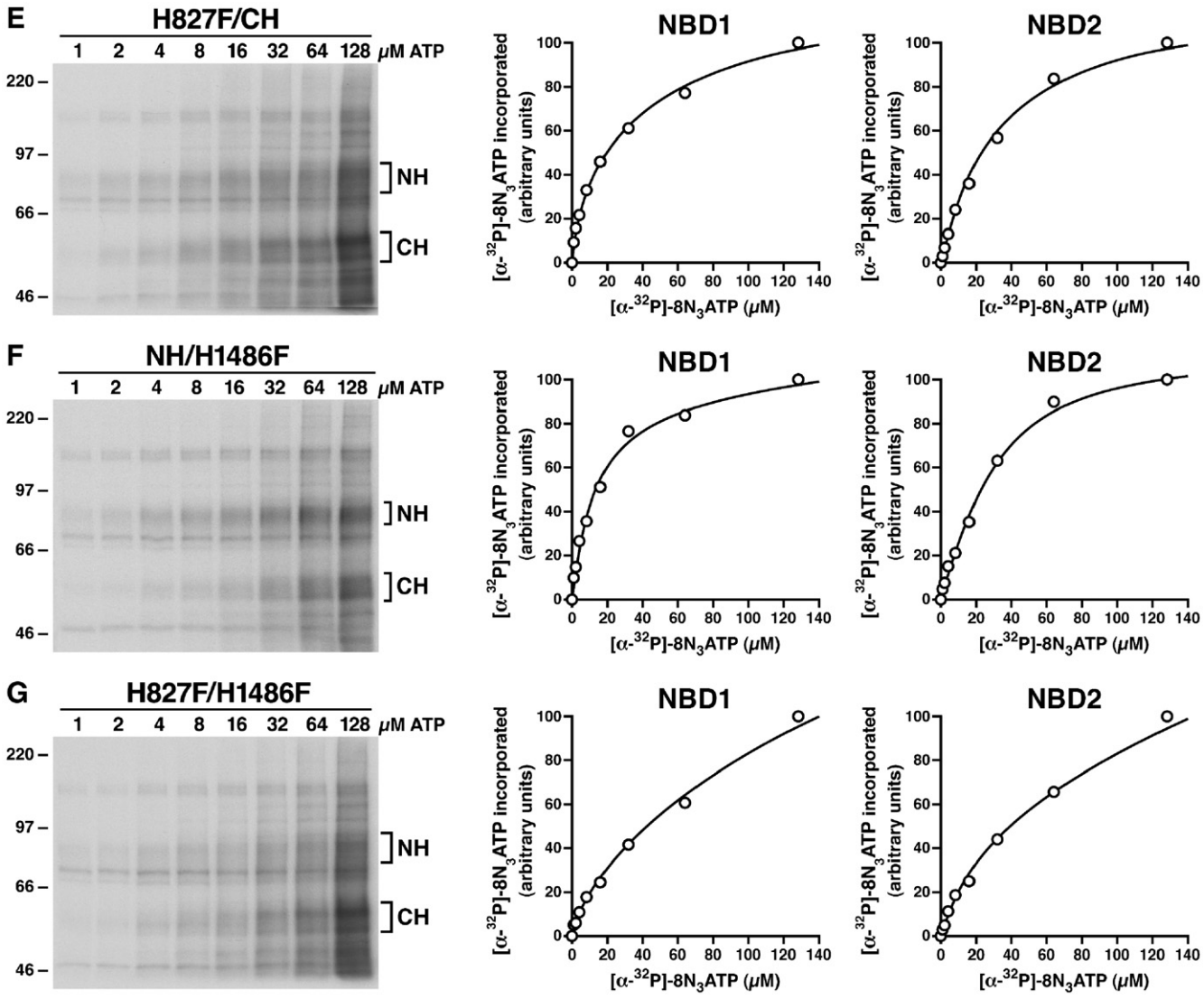

Fig. 2 (*continued*).

efficiently hydrolyzed, we were not sure whether this was caused by mis-folding of the protein introduced by the mutation or by preventing hydrogen-bond formation between the residue at 1486 and the γ-phosphate of the bound ATP or the putative catalytic base. Since complex-glycosylated form of membrane-bound protein in mammalian cells was used as a criterion to indicate that the membrane glycoprotein was globally folded properly, the H827L, H1486L, H827L/H1486L, H827F, H1486F and H827F/H1486F mutations were introduced into full length of MRP1 cDNA in pNUT/MRP1/His [31] and expressed in BHK cells at 37 °C. The results in Fig. 4A clearly indicate that all of these mutants form complex-glycosylated mature proteins at 37 °C, ruling out the former possibility. However, the amount of H827L/H1486L or H827F/H1486F double-mutated MRP1 is slightly less than that of wild-type MRP1 (Fig. 4A), implying that these double mutants might affect the stability of the protein in BHK cells. Regardless of whether these mutants would affect the protein stability or not, the in vitro functional analyses by using membrane vesicles

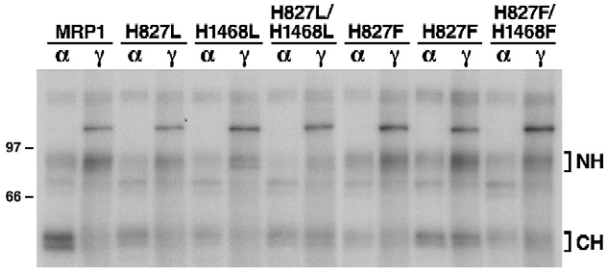

Fig. 3. Substitution of H1486 with either a leucine (L) or a phenylalanine (F) decreased the rate of ATP hydrolysis at the mutated NBD2. Membrane vesicles were prepared from Sf21 cells infected with viral particles containing either wild-type or variant mutants of human MRP1. Photolabeling experiments were carried out in a 10 μl of solution containing 10 μg membrane vesicle proteins, 800 μM vanadate and 10 μM of either [α-^{32}P]-8-N_3ATP (α) or [γ-^{32}P]-8-N_3ATP (γ) at 37 °C for 2 min. The reaction mixture was brought back to ice, UV-irradiated on ice for 2 min, subjected to SDS-PAGE (7%) and electroblotted to a nitrocellulose membrane. Molecular weight markers are indicated on the left. NH and CH on the right of the gel indicate the ^{32}P-8-N_3ATP labeled N-half and C-half of MRP1 proteins.

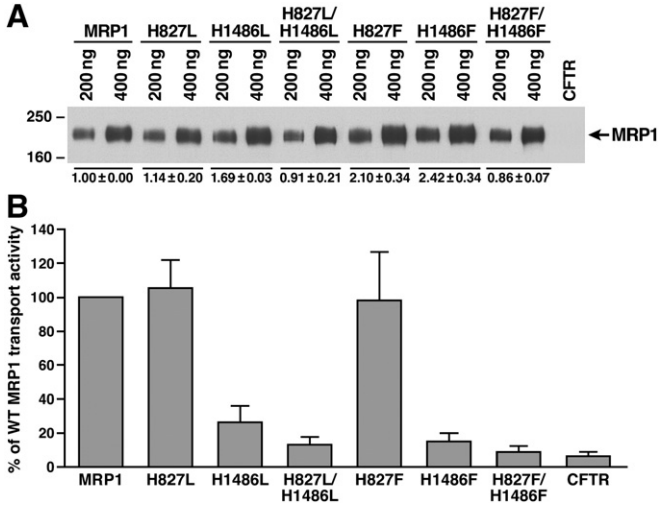

Fig. 4. Prevention of hydrogen bond formation of the residue at 1486 in NBD2 with the γ-phosphate of the bound ATP and the putative catalytic base in this site significantly decreased the ATP-dependent LTC4 transport activity. (A) Expression of wild-type and variant mutants (shown on top of the gel) of full length human MRP1 proteins in BHK cells at 37 °C. Membrane vesicles were prepared from BHK cells expressing either wild-type or variant mutants of human MRP1. The amounts of membrane vesicle protein loaded are indicated on the top of the gel. Molecular weight markers are indicated on the left. MRP1 on the right indicates the 190 kDa complex-glycosylated human MRP1 proteins that were detected in western blot by employing the monoclonal antibody 42.4. The intensities of the 190 kDa bands were determined by a scanning densitometer. The mean ratios (n=3), considering the amount of wild type MRP1 as 1, of the mutant proteins are listed at the bottom of the gel. (B) Relative rate of ATP-dependent LTC4 transport activity. The assays were carried out in a 30 μl solution containing 3 μg of membrane vesicles (the amount of MRP1 protein determined in A was adjusted to a similar amount by adding varying amount of membrane vesicles prepared from BHK cells transfected with human CFTR cDNA and 4 mM AMP (used as a control) or 4 mM ATP at 37 °C for 4 min. The amount of LTC4 bound to the membrane vesicles in the presence of 4 mM AMP was subtracted from the corresponding samples in the presence of 4 mM ATP. The data are means±S.D. of four triplicate-determinations.

containing these mutants should reflect the effects of these mutations on the protein function. The ATP-dependent LTC4 transport activities (Fig. 4B) of these full-length mutants, including H827L, H1486L, H827L/H1486L, H827F, H1486F and H827F/H1486F, are consistent with the results derived from N-half+C-half (Fig. 1C), reinforcing the conclusions made in Figs. 1, 2 and 3.

3.5. Hydrogen-bond formation of the residue at 1486 with the γ-phosphate of the bound ATP and other residues, such as putative catalytic base E1455, plays a crucial role during the ATP-dependent solute transport by MRP1

If hydrogen-bond formation between the residue at 1486 and the γ-phosphate of the bound ATP and the putative catalytic base plays such an important role during ATP hydrolysis at NBD2, substitution of the H residue in H-loop with amino acid residues, such as D, N, E, Q, Y or W, that may potentially form hydrogen-bonds with these components might rescue the ATP-dependent LTC4 transport activity. In order to test this hypothesis, H827D, H1486D, H827D/H1486D, H827N, H1486N, H827N/H1486N, H827E, H1486E, H827E/H1486E, H827Q, H1486Q, H827Q/H1486Q, H827Y, H1486Y, H827Y/H1486Y, H827W, H1486W and H827W/H1486W mutations (Fig. 5A) were introduced into full length of MRP1 cDNA in pNUT/MRP1/His and expressed in BHK cells at 37 °C. The results in Fig. 5B indicate that all these mutants form complex-glycosylated mature MRP1 proteins in BHK cells at 37 °C. Consistent with the H827L or H827F mutation in NBD1, all of the NBD1 mutants, including H827D, H827N, H827E, H827Q, H827Y and H827W, have transport activities similar to that of wild-type MRP1 (Fig. 5C), implying that no matter whether or not these NBD1 mutants form hydrogen-bonds with these components, none of them has a significant effect on the ATP hydrolysis at the un-mutated NBD2 and the ATP-dependent solute transport. However, in contrast, mutations in NBD2 have variant effects on the ATP-dependent solute transport (Fig. 5C). For example, H1486Q had similar transport activity (112%) as that of wild-type MRP1 (Fig. 5C), whereas H1486E dropped this activity to ~36% of the wild-type (Fig. 5C). H1486N had ~60% of wild-type MRP1 transport activity, whereas H1486D dropped this activity to ~20%. Interestingly, although H1486F dropped this transport activity to ~15%, substitution of the

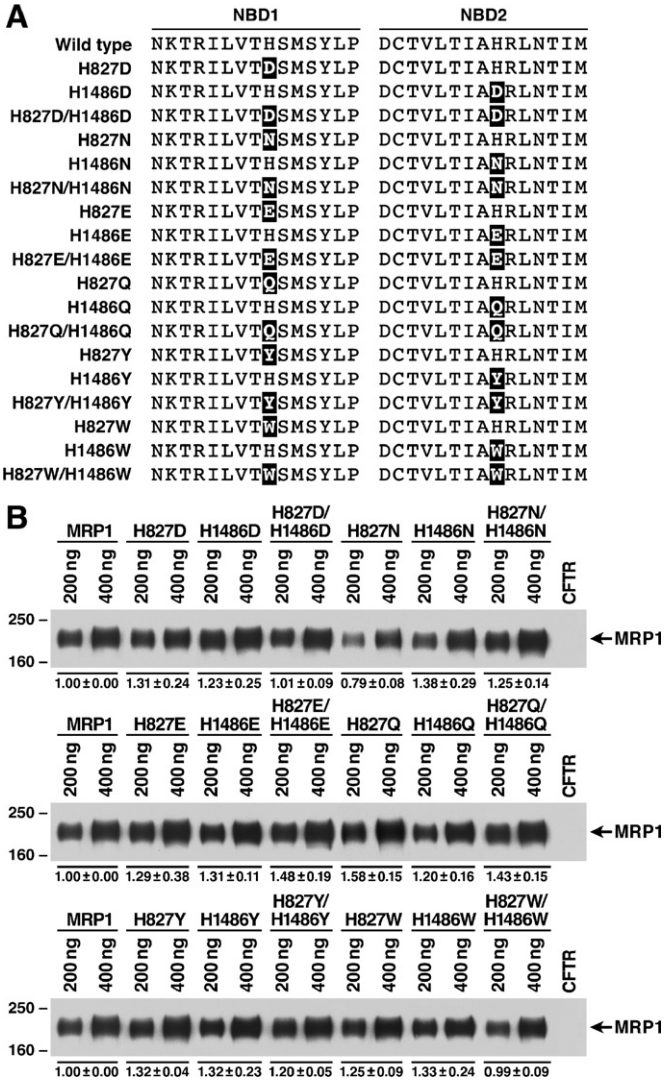

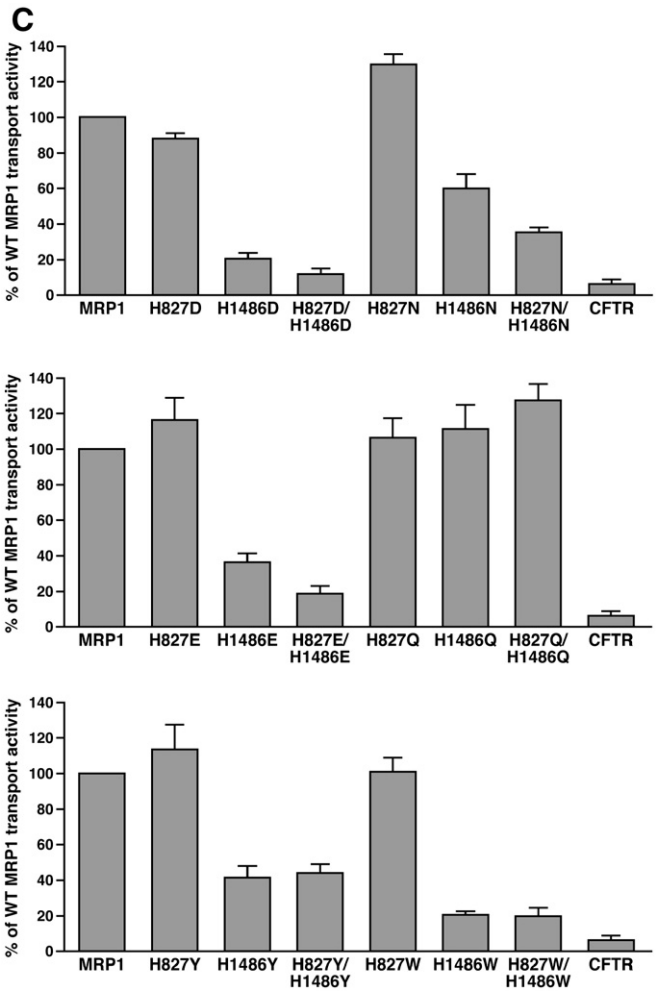

Fig. 5. Hydrogen-bond formation of the residue at 1486 with the γ-phosphate of the bound ATP and the putative catalytic base in this site plays a crucial role in ATP-dependent solute transport. (A) Substitution of the histidine residue at 827 or 1486 with variant amino acids, including D, N, E, Q, Y and W, that may potentially form hydrogen-bond with the γ-phosphate of the bound ATP and putative catalytic base in NBD2. The highlighted letters indicate that the H residue at that position was substituted with D, N, E, Q, Y or W. (B) Expression of wild-type and variant mutants of full length human MRP1 proteins in BHK cells at 37 °C. Membrane vesicles were prepared from BHK cells transfected with either wild-type or mutants and used to do western blot by employing the NBD1-specific monoclonal antibody 42.4 [20]. The amounts of membrane vesicle protein loaded in the gel are indicated on top of the gel. Molecular weight markers are indicated on the left. MRP1 on the right indicates the 190 kDa complex-glycosylated human MRP1 proteins. The intensities of the 190 kDa bands were determined by a scanning densitometer. The mean ratios ($n=3$), considering the amount of wild type MRP1 as 1, of the mutant proteins are listed at the bottom of the gel. (C) Relative rate of ATP-dependent LTC4 transport activity. The assays were carried in the same way as described in Fig. 4. The data are means±S.D. of four triplicate-determinations.

H1486 with a Y residue, which has an extra hydroxyl group on the benzene ring of F residue that might potentially form hydrogen-bonds with the γ-phosphate of the bound ATP and the putative catalytic base E1455, increased this transport activity from 15% to 42% (Fig. 5C). In contrast, substitution of this H residue in H-loop with another aromatic W residue (H1486W), which might also form the hydrogen-bond between the nitrogen atom in the ring structure of tryptophan and the γ-phosphate of the bound ATP and the putative catalytic base E1455, dropped this transport activity to ~21% (Fig. 5C). In addition, the transport activities of the double mutants are either similar to or less active than the corresponding NBD2 mutants (Fig. 5C), implying that mutations at NBD2 play a dominant role for the ATP-dependent solute transport.

4. Discussion

ATP binding to NBD1 of MRP1 induced conformational changes of the protein and enhanced nucleotide binding at NBD2 [22]. If the stereo-structure of a nucleotide is altered, nucleotide binding to NBD1 may not induce the proper conformational changes that enhance the nucleotide binding at NBD2. For example, the angle of P–N–P in AMP–PNP is slightly different from that of P–O–P in ATP, in other words, the relative location of the γ-phosphate or the stereo-structure of AMP–PNP is different from that of ATP. Although AMP–PNP can bind to NBD1 of MRP1, this binding cannot enhance the AMP–PNP binding or vanadate-dependent ADP trapping to NBD2 [22,40], implying that precise stereo-interactions between the residues in MRP1 and the bound nucleotide are required to induce the proper conformational changes of the protein. Nucleotide binding to NBD1 and NBD2 may be sufficient to transport the bound substrate LTC4 from high affinity site to low affinity site [30]. However, this translocation also requires proper stereo-structure of a nucleotide. For example, ATPγS binding to MRP1 can transport the bound LTC4 from high to low affinity site whereas AMP–PNP cannot [30]. Accordingly, this translocation also requires proper stereo-structures of the NBDs of MRP1. For example, ATP binding to wild-type MRP1 can transport the bound LTC4 from high to low affinity site whereas ATP binding to the K684R- or the D1454N-mutated MRP1 cannot [30].

H827L-, H827F-, H827D-, H827N-, H827E-, H827Q-, H827Y- and H827W-mutated MRP1 form complex glycosylated mature protein in BHK cells at 37 °C (Figs. 4A and 5B), implying that these mutations in NBD1 did not significantly alter the protein conformation. In addition, BHK cells expressing H827L-mutated MRP1 exerted similar resistance to daunomycin as wild-type (data not shown), implying that H827L-mutated MRP1 was properly routed to the plasma membrane. These NBD1 mutants, regardless of whether they were expressed in the form of N-half+C-half in Sf21 cells or full length in BHK cells, did not significantly affect the ATP-dependent LTC4 transport activity (Figs. 1C, 4B and 5C), implying that these mutations in NBD1 did not have significant effects on ATP hydrolysis at the un-mutated NBD2. Since some of these mutations, such as H827L or H827F, definitely prevent formation of the hydrogen-bonds of the residue at 827 with the γ-phosphate of the bound ATP [28,34,41–43], it is reasonable to predict that these mutations would decrease the affinity for ATP at the mutated NBD1. Indeed, H827L mutation significantly increased the K_d (8-N_3ATP) values of the mutated NBD1 (Fig. 2 and Table 1) and the un-mutated NBD2 (Fig. 2 and Table 1), implying that hydrogen-bond formation between the residue

at H827 and the γ-phosphate of the bound ATP may contribute to ATP binding. However, in contrast, H827F mutation did not significantly affect the K_d (8-N_3ATP) values of the mutated NBD1 and the un-mutated NBD2 (Fig. 2 and Table 1). These results were interpreted as that: (1) proper conformation of the ATP binding pocket may play a major role for ATP binding, whereas hydrogen-bond formation between the residue at 827 and the γ-phosphate of the bound ATP may play a minor role for ATP binding; (2) H827L mutation may induce micro-conformational changes in ATP binding pocket that decrease affinity for ATP at the mutated NBD1 and then subsequently at the un-mutated NBD2; (3) substitution of the five-member imidazole ring in histidine with six-member benzene ring in phenylalanine definitely prevented formation of hydrogen bonds with the γ-phosphate of the bound ATP and the putative catalytic base D793, but retained van der Waals interactions with the residues in D-loop of NBD2 [29]. Interestingly, structural analysis of recombinant human MRP1-NBD1 revealed that the "catalytic dyad" formed between D793 and H827 pointed away from the γ-phosphate of the bound ATP in this site [45], implying that H827 may not form hydrogen-bond with the γ-phosphate of the bound ATP. This orientation also explained why NBD1 of human MRP1 protein has low ATPase activity [19,20]. Since mutations of H827L and H827F also prevent the formation of this "catalytic dyad" between D793 and L827 or F827, fully functional H827L- or H827F-mutated MRP1 suggests that formation of the "catalytic dyad" between D793 and H827 is not important for MRP1 function. In addition, since none of these NBD1 mutants significantly affects the ATP-dependent LTC4 transport (Figs. 1C, 4B and 5C), it means that ATP binding to these mutated NBD1s still stimulates nucleotide binding at the un-mutated NBD2 [22].

In contrast, mutations in NBD2, such as H1486L, H1486F, H1486D, H1486N, H1486E, H1486Q, H1486Y and H1486W, have variant effects on the ATP-dependent LTC4 transport (Figs. 1C, 4B and 5C)). Substitution of the H1486 in H-loop with residues that would not form hydrogen-bond with the γ-phosphate of the bound ATP in NBD2, including H1486L-, H1486F-, H827L/H1486L- or H827F/H1486F-mutated MRP1, severely impaired the ATP-dependent LTC4 transport, presumably because the bound ATP at the mutated NBD2 (Fig. 2C, D, F and G) were not efficiently hydrolyzed (Fig. 3 and Table 2). These results reinforce our conclusion that ATP hydrolysis at NBD2 plays a crucial role for ATP-dependent solute transport [21]. However, why H1486F mutation did not significantly affect 8-N_3ATP binding (Fig. 2F and Table 1) but severely impaired the ATP hydrolysis at the mutated NBD2 (Fig. 3 and Table 2) was not well understood. These results were interpreted as that replacement of the imidazole ring in histidine with benzene ring in phenylalanine did not lose the ability to interact with the residues in D-loop of NBD1 via van der Waals interactions [29] and kept the NBD1·ATP·ATP·NBD2 sandwich structure intact, but lost ability to form hydrogen bond with the γ-phosphate of the bound ATP [28,34,41–43] and to form "catalytic dyad" with the putative catalytic base E1455 [29,45]. The only difference between H1486F and H1486Y is that H1486Y has an extra hydroxyl group on the benzene ring. H1486F mutation almost abolished the ATP-dependent LTC4 transport activity completely (Figs. 1C and 4B), whereas H1486Y mutation retained ~41% of wild-type LTC4 transport activity (Fig. 5C), presumably the hydroxyl group on the benzene ring of tyrosine provides a possibility to form hydrogen-bond with the γ-phosphate of the bound ATP. This means that hydrogen-bond formation between the residue at 1486 and the γ-phosphate of the bound ATP may play a very important role during ATP hydrolysis. The above results could also be interpreted as that the hydroxyl group on the benzene ring of tyrosine provides a possibility to form a "catalytic dyad" with the putative catalytic base E1455. This means that the "catalytic dyad" formation may also play a very important role during ATP hydrolysis.

Regardless of which mechanism plays an important role, substitution of this histidine residue with an amino acid that would potentially prevent formation the hydrogen bond between the residue in H-loop and the γ-phosphate of the bound ATP or the putative catalytic base should severely impair the ATP hydrolysis at the mutated site. Indeed, several substitutions of this histidine residue in H-loop with amino acids that prevented formation of hydrogen bonds severely impaired the ATP hydrolysis and ATP-dependent solute transport. For example, substitution of H211 in HisP with an arginine residue did not significantly affect ATP binding [46], but the H211R mutant neither supported ATP hydrolysis nor histidine translocation [46,47]; replacement of H662 in HlyB with an alanine residue completely abolished the ATPase activity [44]; substitution of H192 in MalK with an arginine residue abolished ATP hydrolysis [48] and ATP-dependent maltose uptake [48,49].

In contrast, substitution of the histidine residue in H-loop with an amino acid that might potentially form the hydrogen-bonds should support the ATP hydrolysis and ATP-dependent solute transport. Indeed, H1486Q-mutated MRP1 is fully active (Fig. 5C), implying that the hydrogen-bond formations between Q1486 and the γ-phosphate of the bound ATP or the putative catalytic base E1455 are as strong as in wild-type. However, H1486E exerts ~36% of wild-type MRP1 transport activity (Fig. 5C), presumably the carboxyl group of E1486 cannot form strong hydrogen-bonds with the γ-phosphate of the bound ATP and the putative catalytic base E1455 in NBD2. Accordingly, although H1486N has the same side group as the H1486Q mutation, except that the length of the side chain in H1486N is one carbon (or 1.541 Å) shorter than in H1486Q, the transport activity of H1486N dropped from ~112% (H1486Q) to ~60% (Fig. 5C), implying that the distance between two groups forming hydrogen-bond also plays an important role. The transport activity of H1486D dropped from ~36% (H1486E) to ~20% (Fig. 5C), consistent with the above conclusion. In addition, substitution of H587 or H1232 in P-gp with a Q residue did not significantly affect the ATPase activity of the protein, whereas substitution of H587 or H1232 with an alanine residue completely abolished the ATPase activity (Suresh Ambudkar, personal communication), reinforced our above hypothesis.

Interestingly, the ATP-dependent LTC4 transport activities of the double mutants, including H827L/H1486L, H827F/H1486F, H827L/H1486L, H827F/H1486F, H827L/H1486L,

H827F/H1486F, H827L/H1486L and H827F/H1486F, are either similar to or lower than their corresponding mutations in NBD2 (Figs. 4B and 5C), supporting our conclusion that ATP hydrolysis at NBD2 plays a crucial role for ATP-dependent solute transport by MRP1 [21].

Acknowledgments

We thank Irene Beauvais for preparation of the manuscript and Marv Ruona for preparation of the graphics.

This work was supported by the Grant CA89078 from the National Cancer Institute, National Institutes of Health (CA89-078, Xiu-bao Chang).

References

[1] R.L. Juliano, V. Ling, A surface glycoprotein modulating drug permeability in Chinese hamster ovary cell mutants, Biochim. Biophys. Acta 455 (1976) 152–162.
[2] C.J. Chen, J.E. Chin, K. Ueda, D.P. Clark, I. Pastan, M.M. Gottesman, I.B. Roninson, Internal duplication and homology with bacterial transport proteins in the mdr1 (P-glycoprotein) gene from multidrug-resistant human cells, Cell 47 (1986) 381–389.
[3] R. Allikmets, L.M. Schriml, A. Hutchinson, V. Romano-Spica, M. Dean, A human placenta-specific ATP-binding cassette gene (ABCP) on chromosome 4q22 that is involved in multidrug resistance, Cancer Res. 58 (1998) 5337–5339.
[4] L.A. Doyle, W. Yang, L.V. Abruzzo, T. Krogmann, Y. Gao, A.K. Rishi, D.D. Ross, A multidrug resistance transporter from human MCF-7 breast cancer cells, Proc. Natl. Acad. Sci. U. S. A. 95 (1998) 15665–15670.
[5] S.E. Mirski, J.H. Gerlach, S.P. Cole, Multidrug resistance in a human small cell lung cancer cell line selected in adriamycin, Cancer Res. 47 (1987) 2594–2598.
[6] S.P. Cole, G. Bhardwaj, J.H. Gerlach, J.E. Mackie, C.E. Grant, K.C. Almquist, A.J. Stewart, E.U. Kurz, A.M. Duncan, R.G. Deeley, Overexpression of a transporter gene in a multidrug-resistant human lung cancer cell line [see comments], Science 258 (1992) 1650–1654.
[7] J.H. Gerlach, J.A. Endicott, P.F. Juranka, G. Henderson, F. Sarangi, K.L. Deuchars, V. Ling, Homology between P-glycoprotein and a bacterial haemolysin transport protein suggests a model for multidrug resistance, Nature 324 (1986) 485–489.
[8] P. Gros, J. Croop, D. Housman, Mammalian multidrug resistance gene: complete cDNA sequence indicates strong homology to bacterial transport proteins, Cell 47 (1986) 371–380.
[9] E. Bakos, T. Hegedus, Z. Hollo, E. Welker, G.E. Tusnady, G.J. Zaman, M.J. Flens, A. Varadi, B. Sarkadi, Membrane topology and glycosylation of the human multidrug resistance-associated protein, J. Biol. Chem. 271 (1996) 12322–12326.
[10] D.R. Hipfner, K.C. Almquist, E.M. Leslie, J.H. Gerlach, C.E. Grant, R.G. Deeley, S.P. Cole, Membrane topology of the multidrug resistance protein (MRP). A study of glycosylation-site mutants reveals an extracytosolic NH2 terminus, J. Biol. Chem. 272 (1997) 23623–23630.
[11] K. Miyake, L. Mickley, T. Litman, Z. Zhan, R. Robey, B. Cristensen, M. Brangi, L. Greenberger, M. Dean, T. Fojo, S.E. Bates, Molecular cloning of cDNAs which are highly overexpressed in mitoxantrone-resistant cells: demonstration of homology to ABC transport genes, Cancer Res. 59 (1999) 8–13.
[12] T. Litman, M. Brangi, E. Hudson, P. Fetsch, A. Abati, D.D. Ross, K. Miyake, J.H. Resau, S.E. Bates, The multidrug-resistant phenotype associated with overexpression of the new ABC half-transporter, MXR (ABCG2), J. Cell Sci. 113 (Pt. 11) (2000) 2011–2021.
[13] K. Kage, S. Tsukahara, T. Sugiyama, S. Asada, E. Ishikawa, T. Tsuruo, Y. Sugimoto, Dominant-negative inhibition of breast cancer resistance protein as drug efflux pump through the inhibition of S–S dependent homodimerization, Int. J. Cancer 97 (2002) 626–630.
[14] L.A. Doyle, D.D. Ross, Multidrug resistance mediated by the breast cancer resistance protein BCRP (ABCG2), Oncogene 22 (2003) 7340–7358.
[15] T. Nakanishi, L.A. Doyle, B. Hassel, Y. Wei, K.S. Bauer, S. Wu, D.W. Pumplin, H.B. Fang, D.D. Ross, Functional characterization of human breast cancer resistance protein (BCRP, ABCG2) expressed in the oocytes of *Xenopus laevis*, Mol. Pharmacol. 64 (2003) 1452–1462.
[16] B. Han, J.T. Zhang, Multidrug resistance in cancer chemotherapy and xenobiotic protection mediated by the half ATP-binding cassette transporter ABCG2, Curr. Med. Chem. Anti-Cancer Agents 4 (2004) 31–42.
[17] O. Polgar, R.W. Robey, K. Morisaki, M. Dean, C. Michejda, Z.E. Sauna, S.V. Ambudkar, N. Tarasova, S.E. Bates, Mutational analysis of ABCG2: role of the GXXXG motif, Biochemistry 43 (2004) 9448–9456.
[18] Q. Mao, J.D. Unadkat, Role of the breast cancer resistance protein (ABCG2) in drug transport, AAPS J. 7 (2005) E118–E133.
[19] M. Gao, H.R. Cui, D.W. Loe, C.E. Grant, K.C. Almquist, S.P. Cole, R.G. Deeley, Comparison of the functional characteristics of the nucleotide binding domains of multidrug resistance protein 1, J. Biol. Chem. 275 (2000) 13098–13108.
[20] Y. Hou, L. Cui, J.R. Riordan, X.B. Chang, Allosteric interactions between the two non-equivalent nucleotide binding domains of multidrug resistance protein MRP1, J. Biol. Chem. 275 (2000) 20280–20287.
[21] R. Yang, L. Cui, Y.-X. Hou, J.R. Riordan, X.B. Chang, ATP binding to the first nucleotide binding domain of multidrug resistance-associated protein plays a regulatory role at low nucleotide concentration, whereas ATP hydrolysis at the second plays a dominant role in ATP-dependent leukotriene C4 transport, J. Biol. Chem. 278 (2003) 30764–30771.
[22] Y.X. Hou, L. Cui, J.R. Riordan, X.B. Chang, ATP binding to the first nucleotide-binding domain of multidrug resistance protein MRP1 increases binding and hydrolysis of ATP and trapping of ADP at the second domain, J. Biol. Chem. 277 (2002) 5110–5119.
[23] F. Buyse, Y.X. Hou, C. Vigano, Q. Zhao, J.M. Ruysschaert, X.B. Chang, Replacement of the positively charged Walker A lysine residue with a hydrophobic leucine residue and conformational alterations caused by this mutation in MRP1 impair ATP binding and hydrolysis, Biochem. J. 397 (2006) 121–130.
[24] J.E. Moody, L. Millen, D. Binns, J.F. Hunt, P.J. Thomas, Cooperative, ATP-dependent association of the nucleotide binding cassettes during the catalytic cycle of ATP-binding cassette transporters, J. Biol. Chem. 277 (2002) 21111–21114.
[25] L.F. Payen, M. Gao, C.J. Westlake, S.P. Cole, R.G. Deeley, Role of carboxylate residues adjacent to the conserved core Walker B motifs in the catalytic cycle of multidrug resistance protein 1 (ABCC1), J. Biol. Chem. 278 (2003) 38537–38547.
[26] R. Yang, A. McBride, Y.X. Hou, A. Goldberg, X.B. Chang, Nucleotide dissociation from NBD1 promotes solute transport by MRP1, Biochim. Biophys. Acta 1668 (2005) 248–261.
[27] Q. Zhao, X.B. Chang, Mutation of the aromatic amino acid interacting with adenine moiety of ATP to a polar residue alters the properties of multidrug resistance protein 1, J. Biol. Chem. 279 (2004) 48505–48512.
[28] P.C. Smith, N. Karpowich, L. Millen, J.E. Moody, J. Rosen, P.J. Thomas, J.F. Hunt, ATP binding to the motor domain from an ABC transporter drives formation of a nucleotide sandwich dimer, Mol. Cell 10 (2002) 139–149.
[29] J. Zaitseva, S. Jenewein, T. Jumpertz, I.B. Holland, L. Schmitt, H662 is the linchpin of ATP hydrolysis in the nucleotide-binding domain of the ABC transporter HlyB, EMBO J. 24 (2005) 1901–1910.
[30] L. Payen, M. Gao, C. Westlake, A. Theis, S.P. Cole, R.G. Deeley, Functional interactions between nucleotide binding domains and leukotriene c4 binding sites of multidrug resistance protein 1 (ABCC1), Mol. Pharmacol. 67 (2005) 1944–1953.
[31] X.B. Chang, Y.X. Hou, J.R. Riordan, ATPase activity of purified multidrug resistance-associated protein [published erratum appears in J Biol Chem 1998 Mar 27;273(13):7782], J. Biol. Chem. 272 (1997) 30962–30968.
[32] I. Leier, G. Jedlitschky, U. Buchholz, D. Keppler, Characterization of the ATP-dependent leukotriene C4 export carrier in mastocytoma cells, Eur. J. Biochem. 220 (1994) 599–606.
[33] D.W. Loe, K.C. Almquist, R.G. Deeley, S.P. Cole, Multidrug resistance protein (MRP)-mediated transport of leukotriene C4 and chemotherapeutic

agents in membrane vesicles. Demonstration of glutathione-dependent vincristine transport, J. Biol. Chem. 271 (1996) 9675–9682.
[34] L.W. Hung, I.X. Wang, K. Nikaido, P.Q. Liu, G.F. Ames, S.H. Kim, Crystal structure of the ATP-binding subunit of an ABC transporter, Nature 396 (1998) 703–707.
[35] J. Chen, G. Lu, J. Lin, A.L. Davidson, F.A. Quiocho, A tweezers-like motion of the ATP-binding cassette dimer in an ABC transport cycle, Mol. Cell 12 (2003) 651–661.
[36] E. Balzi, M. Wang, S. Leterme, L. Van Dyck, A. Goffeau, PDR5, a novel yeast multidrug resistance conferring transporter controlled by the transcription regulator PDR1, J. Biol. Chem. 269 (1994) 2206–2214.
[37] J. Trowsdale, I. Hanson, I. Mockridge, S. Beck, A. Townsend, A. Kelly, Sequences encoded in the class II region of the MHC related to the 'ABC' superfamily of transporters, Nature 348 (1990) 741–744.
[38] M.S. Szczypka, J.A. Wemmie, W.S. Moye-Rowley, D.J. Thiele, A yeast metal resistance protein similar to human cystic fibrosis transmembrane conductance regulator (CFTR) and multidrug resistance-associated protein, J. Biol. Chem. 269 (1994) 22853–22857.
[39] J.R. Riordan, J.M. Rommens, B. Kerem, N. Alon, R. Rozmahel, Z. Grzelczak, J. Zielenski, S. Lok, N. Plavsic, J.L. Chou, et al., Identification of the cystic fibrosis gene: cloning and characterization of complementary DNA, Science 245 (1989) 1066–1073.
[40] Y.X. Hou, J.R. Riordan, X.B. Chang, ATP binding, not hydrolysis, at the first nucleotide-binding domain of multidrug resistance-associated protein MRP1 enhances ADP.Vi trapping at the second domain, J. Biol. Chem. 278 (2003) 3599–3605.
[41] G. Lu, J.M. Westbrooks, A.L. Davidson, J. Chen, ATP hydrolysis is required to reset the ATP-binding cassette dimer into the resting-state conformation, Proc. Natl. Acad. Sci. U. S. A. 102 (2005) 17969–17974.
[42] K.P. Hopfner, A. Karcher, D.S. Shin, L. Craig, L.M. Arthur, J.P. Carney, J.A. Tainer, Structural biology of Rad50 ATPase: ATP-driven conformational control in DNA double-strand break repair and the ABC-ATPase superfamily, Cell 101 (2000) 789–800.
[43] K. Diederichs, J. Diez, G. Greller, C. Muller, J. Breed, C. Schnell, C. Vonrhein, W. Boos, W. Welte, Crystal structure of MalK, the ATPase subunit of the trehalose/maltose ABC transporter of the archaeon *Thermococcus litoralis*, EMBO J. 19 (2000) 5951–5961.
[44] J. Zaitseva, S. Jenewein, A. Wiedenmann, H. Benabdelhak, I.B. Holland, L. Schmitt, Functional characterization and ATP-induced dimerization of the isolated ABC-domain of the haemolysin B transporter, Biochemistry 44 (2005) 9680–9690.
[45] O. Ramaen, N. Leulliot, C. Sizun, N. Ulryck, O. Pamlard, J.Y. Lallemand, H. Tilbeurgh, E. Jacquet, Structure of the human multidrug resistance protein 1 nucleotide binding domain 1 bound to Mg2+/ATP reveals a non-productive catalytic site, J. Mol. Biol. 359 (2006) 940–949.
[46] V. Shyamala, V. Baichwal, E. Beall, G.F. Ames, Structure–function analysis of the histidine permease and comparison with cystic fibrosis mutations, J. Biol. Chem. 266 (1991) 18714–18719.
[47] K. Nikaido, G.F. Ames, One intact ATP-binding subunit is sufficient to support ATP hydrolysis and translocation in an ABC transporter, the histidine permease, J. Biol. Chem. 274 (1999) 26727–26735.
[48] A.L. Davidson, S. Sharma, Mutation of a single MalK subunit severely impairs maltose transport activity in *Escherichia coli*, J. Bacteriol. 179 (1997) 5458–5464.
[49] C. Walter, S. Wilken, E. Schneider, Characterization of site-directed mutations in conserved domains of MalK, a bacterial member of the ATP-binding cassette (ABC) family [corrected], FEBS Lett. 303 (1992) 41–44.